J Fluoresc (2016) 26:1579–1590
DOI 10.1007/s10895-016-1842-z

ORIGINAL ARTICLE

Synthesis, Characterization, Electrical Conductivity and Fluorescence Properties of Polyimine Bearing Phenylacetylene Units

Dilek Şenol[1] · **Feyza Kolcu**[1,2] · **İsmet Kaya**[1]

Received: 28 December 2015 / Accepted: 30 May 2016 / Published online: 23 June 2016

Abstract In this study, a Schiff base was synthesized by the condensation reaction of 4-bromobenzaldehyde and 4-aminophenol. Then, phenylacetylene substituted Schiff base monomer (IPA) was obtained by HBr elimination reaction of IPA with phenylacetylene through Sonogashira reaction. IPA was polymerized via chemical oxidative polycondensation reaction. FT-IR and NMR measurements were used for the structural analyses of the synthesized substances. Fluorescence and UV–Vis analyses were carried out for optical characterization. Electrochemical characteristics, electrical conductivities and thermal properties were determined using cyclic voltammetry (CV), four-point probe conductometer, TG-DTA and DSC methods. The main purpose of the present study was to investigate the effects of phenylacetylene bearing units on the properties of conjugated aromatic polyimines. The spectral analysis signified a green light emission behavior when irradiated at different wavelengths. Combined with fluorescent behavior and good thermal stability, the electrical conductivity was found to be very crucial for π-conjugated polymer.

Keywords Imine polymers · Synthesis and characterization · Thermal · Fluorescence properties

✉ Dilek Şenol
dilek_dilek1734@hotmail.com

✉ İsmet Kaya
kayaismet@hotmail.com

[1] Faculty of Sciences and Arts, Department of Chemistry, Polymer Synthesis and Analysis Laboratory, Çanakkale Onsekiz Mart University, 17020 Çanakkale, Turkey

[2] Lapseki Vocational School, Department of Chemistry and Chemical Processing Technologies, Çanakkale Onsekiz Mart University, Çanakkale, Turkey

Introduction

Conducting polymers have already been found widespread use in many, mainly optical and electronic applications such as batteries, displays, plastic wires, optical signal processing, information storage, solar energy conversion, etc. Scientific interest in monosubstituted polyacetylenes, the first synthesized conducting polymers, e.g., poly(ethynylbenzene), as π-conjugated polymers have been rapidly growing for many years and recently focused on the many interesting physicochemical characteristics and novel properties, in particular on conductivity [1, 2], ferromagnetism [3], oxygen permeability [4, 5], humidity sensor [6, 7], nonlinear optical (NLO) materials [8, 9], electroluminescence (EL) materials [10], and so on. Taking this into consideration, imine polymers synthesized in the presence of phenyl acetylene group was targeted to increase the conductivity [11, 12]. Sonogashira reaction is the commonly used method in producing conjugated materials with their potential use in photonic devices. Phenylacetylene oligomers and polymers have semi-conductivity features due to the presence of intense conjugation. The applications of these kinds of materials are used for polarizers, nonlinear optic liquid crystal displays, luminous diodes, thin films, sensors and explosive detection. In addition, they are used in mainly aerospace industry, machine production and rocket techniques because of their resistance to high temperatures. With a view to investigating potential polymers for the aforementioned properties of polyacetylene, a macromolecule with a Nobel Prize, in this study, it is aimed to increase the conductivity in the presence of phenylacetylene group along the imine polymer chain. In addition, water solubility of the synthesized polymer makes it possible to be used in medicine, cosmetic, paint and food industry. Poly(imine)s interact with electron acceptor gases such as iodine with its electron donor feature of its group, leading to the formation of polaron structure thus,

increasing the conductivity of the polymer. By linking acetylene group to the polymer, the conductivity of the polymer is expected to increase. In addition, electrochemical band gap and optical band gap are calculated by determining the HOMO-LUMO values by cyclic voltammetry (CV) and UV–Vis measurements, respectively.

Experimental

Materials

4-bromo benzaldehyde (4BB), 4-aminophenol (4AP), phenyl acetylene (PA), Pd catalysis, cuprous iodide (CuI), triethylamine, tetrabutylammoniumhexafluorophosphate ($TBAPF_6$), N,N-dimethylformamide (DMF), tetrahydrofurane (THF), dimethylsulfoxide (DMSO), methanol, ethanol, acetonitrile (AN), ethyl acetate, diethyl ether, KOH, HCl were supplied by Merck Chemical Co. (Germany) and they were used as received. 30 % aqueous solution of sodium hypochlorite (NaOCl) was supplied by Paksoy Chemical Co. (Turkey).

4-((4-(phenylethynyl)benzylidene)amino)phenol Monomer and its Polymer Synthesis

Schiff base was synthesized by a condensation reaction of equimols of 4-bromobenzaldehyde and 4-aminophenol solved in ethanol and placed into a 100 mL one-necked round bottom flask fitted with a condenser, a thermometer and a magnetic stirrer. The main reaction was maintained for 5 h under reflux at room temperature. The substance was crystallized in acetonitrile and its solvent was evaporated. Coupling was performed by using THF as the solvent, piperidine as a strong base, CuI as a co-catalyzer and $Pd(PPh_3)_4$ as a catalyzer according to Sonogashira reaction in which phenyl acetylene compound was attached to the synthesized Schiff base. Obtained imine-phenylacetylene was put into a 250 mL three-necked round bottom flask and 30 mL distilled water was added. The reaction flask was placed onto the magnetic stirrer with condenser and thermometer. Schiff base was solved by adding KOH (0.1 mol) in the reaction medium. The reaction temperature was increased to 80 °C and 1 mL of 30 % NaOCl solution was added to the environment as the oxidizing agent at regular intervals within 20 min. Reaction mixture became dark brown after adding oxidizing agent. The reaction was maintained for 6 h by stirring with magnetic stirrer. After the reaction, a piece of dark brown solution was transferred into 100 mL beaker and equimolar of 0.1 M HCl solution to KOH used was added to neutralize but, no precipitation was observed. Since there was no precipitated polymer after neutralization, the solvent was just vaporized to get the polymeric product as the potassium salt. Dark colored polymeric product was dried in a vacuum drying-oven at 80 °C for 1 day (Scheme 1). The combinations of the phenylene (C-C) and oxyphenylene (C-O-C) units formed polymer are given in Scheme 2.

IPA: ^{1}H-NMR (DMSO-d_6): δ ppm, 9.49 (s, 1H, -OH), 8.54 (s, 1H, –CH = N), 7.77 (d, 2H, Ar-Hc), 7.64 (d, 2H, Ar-Hf), 7.56 (d, 2H, Ar-Hg), 7.41–7.37 (t, 3H, Ar- Hı, Ar-Hj), 7.13 (d, 2H, Ar-He), 6.72 (d, 2H, Ar-Hb). **IPA:** ^{13}C-NMR (DMSO-d_6): δ ppm, 157.05 (C1-H), 156.38 (C5-H), 142.00 (C6-H), 132.92 (C8-H), 132.29 (C12-H), 130.54 (C13,C14-H), 129.44 (C4,C11-H), 124.75(C9-H), 123.15(C7-H), 120.92 (C3-H), 116.23 (C2-H), 90.10 (C10-H).

PIPA: ^{1}H-NMR (DMSO-d_6): δ ppm, 9.30 (s, 1H, -OH), 8.33 (s, 1H, –CH = N), 7.74 (d, 2H, Ar-Hc), 7.62–7.61 (d, 4H, Ar-Hf, Ar-Hg), 7.51–7.50 (d, 3H, Ar- Hı, Ar-Hj), 7.36 (d, 2H, Ar-He), 6.76 (d, 2H, Ar-Hb). **PIPA:** ^{13}C-NMR (DMSO-d_6): δ ppm, 159.82 (C1-H), 158.66 (C5-H), 156.00 (C-O-C new peak), 151.73(C6-H), 139.31 (C9-H), 138.94 (C = C new peak), 133.65 (C10-H), 131.36 (C12-H)129.28(C2-H), 128.82(C3-H,C13-H,C14-H), 127.32(C4-H, C8-H, C15-H), 124.20 (C11-H), 122.15 (C7-H), 119.96 (C-O-C new peak).

Characterization Techniques

The solubility tests were done in different solvents by using 1 mg sample and 1 ml solvent at 25 °C. The infrared and ultraviolet–visible spectra were measured by PerkinElmer FT-IR Spectrum one and Analytikjena Specord 210 Plus, respectively. The FT-IR spectra were recorded using universal ATR sampling accessory (4000–550 cm^{-1}). ^{1}H and ^{13}C-NMR spectra (Bruker AC FT-NMR spectrometer operating at 400 and 100.6 MHz, respectively) were also recorded by using deuterated DMSO-d_6 and D_2O as solvent at 25 °C. X-ray diffractograms were recorded by a PANalytical empyrean model X-ray diffractometer instrument with $Cu_{K\alpha}$ radiation at a wavelength of 1.54 A^0 over a 2θ range from 5^0 to 90^0 with the scan speed of 4^0 min^{-1}. Scanning electron microscope (SEM) analysis of polymer was obtained by a Jeol JSM-7100 F instrument. The tetramethylsilane was used as internal standard. Thermal data were obtained by using a Perkin Elmer Diamond Thermal Analysis system. TG-DTA measurements were made between 25 and 900 °C (in N_2, rate 10 °C min^{-1}). DSC analyses were carried out between 25 and 450 °C (in N_2, rate 10 °C min^{-1}) by using Perkin Elmer Pyris Sapphire DSC.

Optical and Electrochemical Properties

Ultraviolet–visible (UV–Vis) spectra were measured by Perkin Elmer Lambda 25. The absorption spectra were recorded by using DMSO at 25 °C. The optical band gaps (E_g) were calculated from their absorption edges.

Scheme 1 Synthesis procedures of IPA and PIPA

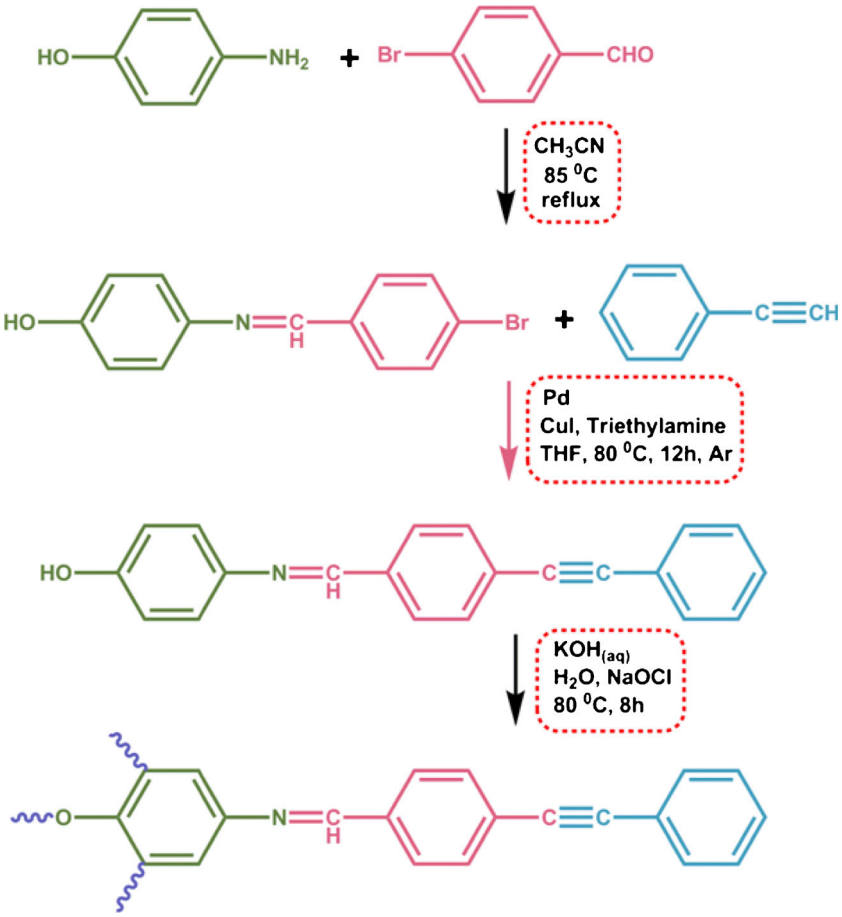

Cyclic voltammetry (CV) measurements were carried out with a CHI 660 C Electrochemical Analyzer (CH Instruments, Texas, USA) at a potential scan rate of 20 mV/s. All the experiments were performed in a dry box filled with argon at room temperature. The electrochemical potential of Ag was calibrated with respect to the ferrocene/ferrocenium (Fc/Fc^{+}) couple. The half-wave potential ($E^{1/2}$) of (Fc/Fc^{+}) was measured in acetonitrile solution of 0.1 M tetrabutylammonium

Scheme 2 The combinations of the phenylene (C-C) and oxyphenylene (C-O-C) units

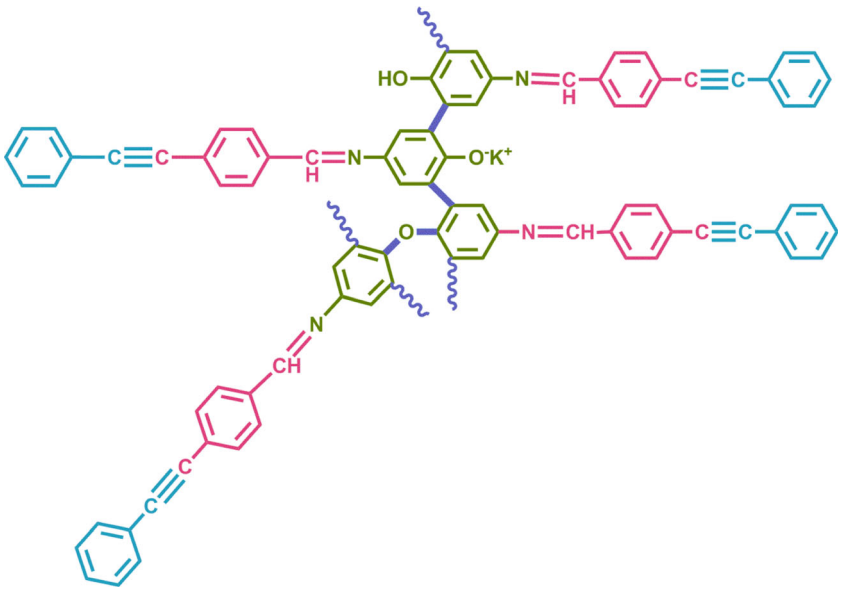

hexafluorophosphate ($TBAPF_6$) and was 0.39 V with respect to Ag wire. The voltammetric measurements were carried out in acetonitrile for the Schiff bases and acetonitrile/DMSO mixture (v/sv:5/1) for the polymers.

Electrical Properties

Conductivities of the synthesized materials were measured on a Keithley 2400 Electrometer. The pellets were pressed on a hydraulic press developing up to 1687.2 kg/cm^2. Iodine doping was carried out by exposing the pellets to iodine vapour at atmospheric pressure and room temperature in a desiccator. The measurements were carried out per 24 h [11, 12].

Fluorescence Measurements

A Shimadzu RF-5301PC spectrofluorophotometer was used in fluorescence measurements. Emission and excitation spectra of the synthesized Schiff base and its polymer were obtained in DMF. Measurements were made in a wide concentration range between 3.125 and 100 mg/L to determine the optimal fluorescence concentrations. Slit width in all measurements was 5 nm.

Computational Method

The electron distribution along the polymer chain for the HOMO-LUMO levels were calculated by using PM3 semi empirical method implemented in Chem Office 2004 version.

Results and Discussion

Solubility of the Compounds

Schiff base polymer containing phenyl acetylene unit was completely soluble in water while it was partially soluble in polar solvents like DMSO and DMF. It was observed that Schiff base was dissolved in all polar solvents.

Spectral Analyses of the Synthesized Compounds

Structures of the synthesized monomer and polymer were explained by FT-IR, UV–Vis, ^{1}HNMR and ^{13}CNMR analyses. Spectra were taken by using Fourier Transform Infrared (FT-IR) Spectrometer (Perkin Elmer FT-IR Spectrum one, with ATR sampling accessory). Characteristic carbonyl peak at 1687 cm^{-1} for 4-bromobenzaldehyde in Fig. 1a, and hydroxyl (-OH) peak at 3341–3282 cm^{-1} and double branch peaks attributed to amine group at 3310 cm^{-1} for 4-aminophenol in Fig. 1b were observed. As a result of Schiff base formation, the loss of amine and hydroxyl protons could be observed as a result of the formation of a broad peak in that area. The formation of imine (-HC = N) was proved by the appearance of a peak at 1619 cm^{-1} as a result of a condensation reaction between aldehyde and amine in the spectrum of Schiff base monomer due to the loss of characteristic peaks of aldehyde and amine (Fig. 1c). Then, the -CH peak for acetylene group at 3290 cm^{-1} was not observed in Fig. 1e when phenyl acetylene was added to the synthesized Schiff base (Fig. 1d). The absorption bands for imine (C = N) at 1619 cm^{-1} and acetylene (C ≡ C) at 2260 cm^{-1} were observed due to the Schiff base monomer structure containing acetylene group (IPA). As seen in Fig. 1f, broadening in the peaks and observation of the absorption bands for the imine and acetylene groups were the indications of a polymer (PIPA) formation.

^{1}H-NMR and ^{13}C-NMR spectrum of the monomer and the polymer were taken at DMSO-d_6, D_2O, respectively. The structures and the chemical shifts of ^{1}H-NMR and ^{13}C-NMR for the monomer (IPA) and its polymer (PIPA) are given in Figs. 2 and 3. ^{1}H-NMR spectrum of IPA monomer gave sharp proton signals as expected. The hydroxyl, azomethine and aromatic proton signals were observed in 9.49, 8.54 and 7.77–6.71 ppm, respectively [13]. In ^{1}H-NMR spectrum of polymer, an increase in the number of the peaks and an enlargement of the peaks were observed. This enlargement was due to the presence of the repeated monomer units with different chemical environments. The observation of a decrease in the intensity and broad peak of hydroxyl group for the polymer indicated that polymerization went through C-O-C coupling. According to the ^{13}C-NMR spectrum of the monomer and polymer, it was observed that the hydroxyl (C-OH) and acetylene (C ≡ C) peaks at 157.05 and 90.02 ppm shifted to 159.82 and 89.00 ppm, respectively. The oxyphenylene (C-O-C) carbon and phenylene (C-C) carbon signals formed due to the imine-acetylene formation were observed at 119.96 and 138.94 ppm, respectively [14]. Since the oxygen atom of hydroxyl group and C2 atom at *ortho* positon possessed the highest propensity in the HOMO level as seen in Fig. 4, the polymer formation was expected via C-O-C and C-C couplings, respectively.

Optical and Electrochemical Properties

According to the UV–Vis spectra of monomer and polymer as seen in Fig. 5, three sharp and one shoulder bands were displayed with λ_{max} values of 290, 308, 330 and 352 nm, respectively. Peak sharpness observed in monomer became broader as a result of the polymer formation, and the formation of a new peak observed at 464 nm for the $n \rightarrow \pi^*$ transition in polymer indicated the increase in conjugation along the polymer chain. λ_{onset} values of the monomer and the polymer were found to be 405 and 450 nm, respectively. E_g values were given in Table 1 as a result of the calculations using the formula of 1242/ $\lambda_{onset.}$ [15]. E_g value of polymer was found to be lower than that of the monomer which was an

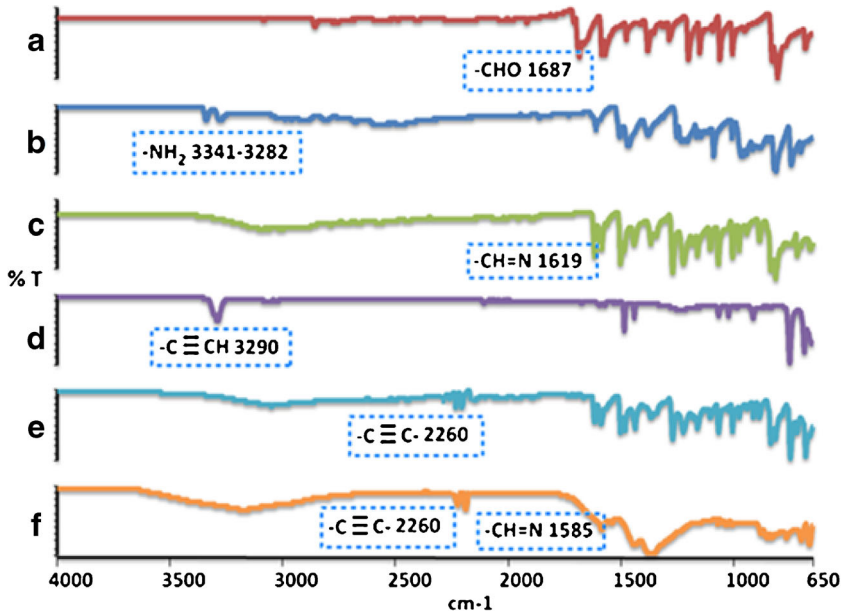

Fig. 1 FT-IR spectra of 4-bromobenzaldehyde (**a**) 4-aminophenol (**b**), Schiff base (**c**), phenyl acetylene (**d**), Schiff base containing acetylene group (**e**), imine polymer containing acetylene group (**f**)

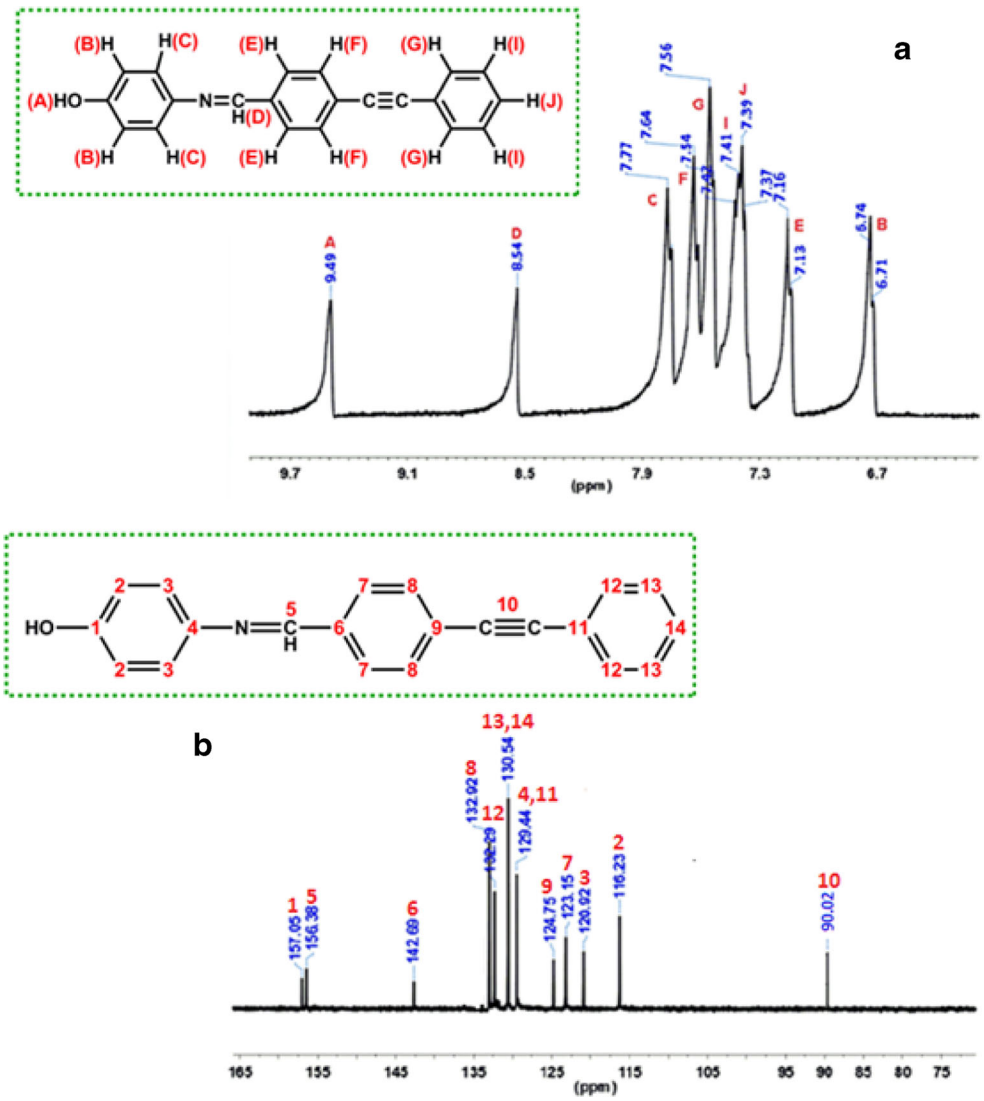

Fig. 2 ^{1}H-NMR (**a**) and ^{13}C-NMR (**b**) spectra of IPA

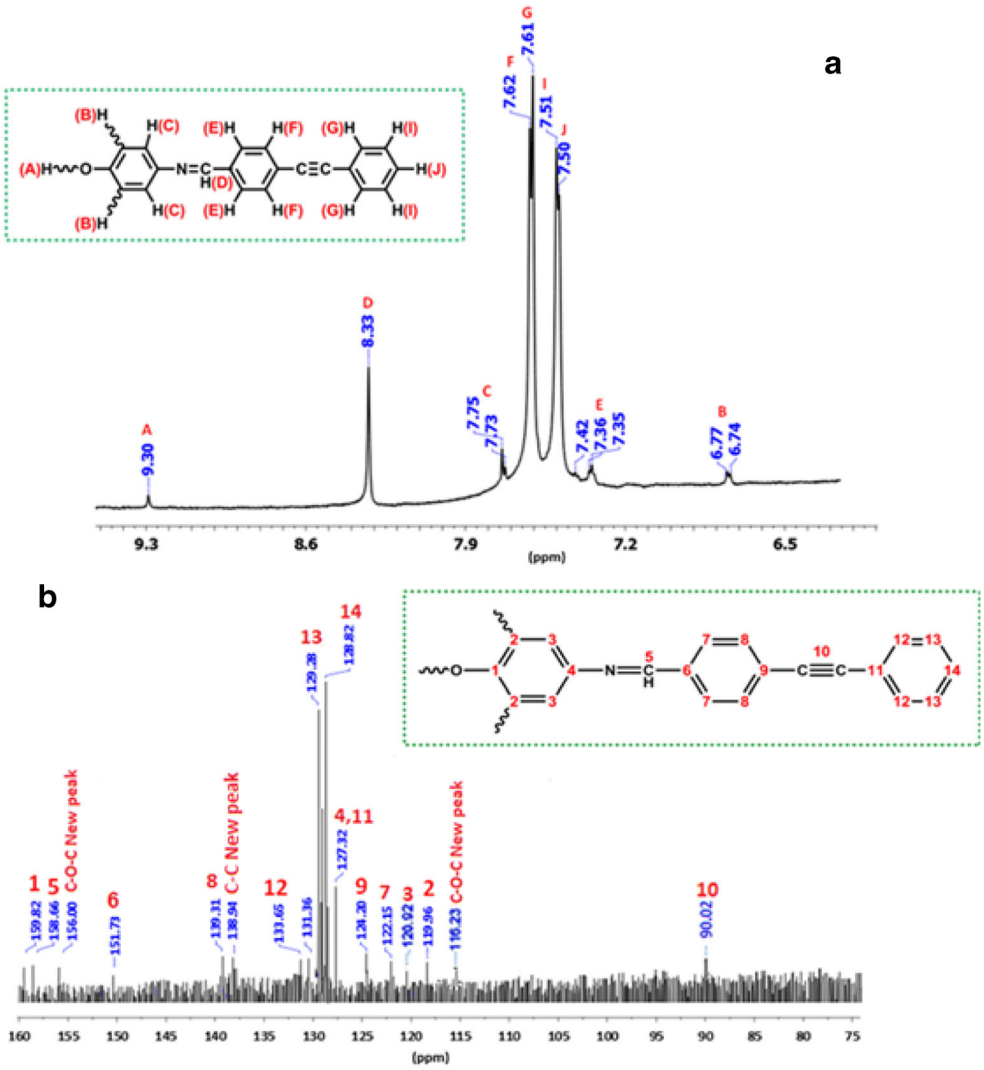

Fig. 3 ^{1}H-NMR (**a**) and ^{13}C-NMR (**b**) spectra of PIPA

indication of increasing conjugation along the polymer chain [16].

Electrochemical properties of the synthesized Schiff base monomer and its polymer were examined by using cyclic voltammetry (CV) technique and the oxidation-reduction peak potentials of potential-current voltammograms for the monomer and its polymer are given in Fig. 6a. While oxidation peak was observed for the hydroxyl group (OH) in positive region for both monomer and polymer in the spectrum, the peaks regarding to the reduction of imine (-HC = N) nitrogen by being protonated were observed in negative region. CVs of the synthesized compounds were taken by using glassy carbon electrode (GCE). The voltammetric measurements were carried out in acetonitrile solution of 0.1 M

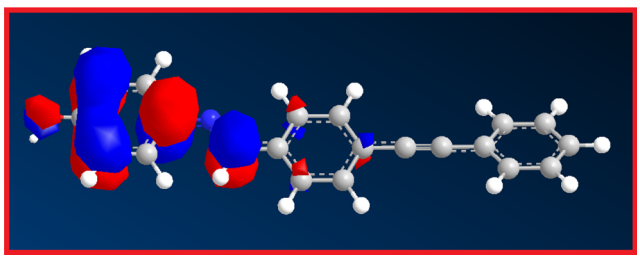

Fig. 4 Graphical representation of the HOMO and LUMO orbitals, together with the optimized molecular structure of PIPA

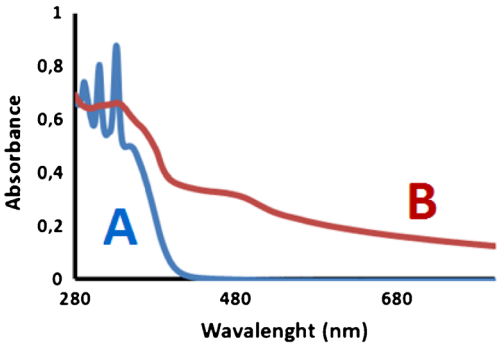

Fig. 5 Absorption spectra of the IPA (**a**) and PIPA (**b**)

Table 1 Electronic structure parameters of the synthesized compounds

Compounds	E_{ox} (V)	E_{Red} (V)	[a]HOMO (eV)	[b]LUMO (eV)	[c]E'_g (eV)	[d]E_g (eV)
IPA	1.61	−1.52	−6.00	−2.87	3.13	3.06
PIPA	1.32	−1.22	−5.71	−3.17	2.54	2.26

[a] Highest occupied molecular orbital

[b] Lowest unoccupied molecular orbital

[c] Electrochemical band gap

[d] Optical band gap

tetrabutylammonium hexafluorophosphate ($TBAPF_6$) and water/$TBAPF_6$ mixture (*v*/*v*:1/3) for the monomer and polymer, respectively. Electrochemical data of the monomer and its polymer are given in Table 1. The HOMO-LUMO energy levels and electrochemical band gaps (E'_g) were figured out from the oxidation and reduction peak potentials [17]. The calculations were made by using the following equations [18, 19]:

$$E_{HOMO} = -(4.39 + E_{ox}) \quad (1)$$

$$E_{LUMO} = -(4.39 + E_{red}) \quad (2)$$

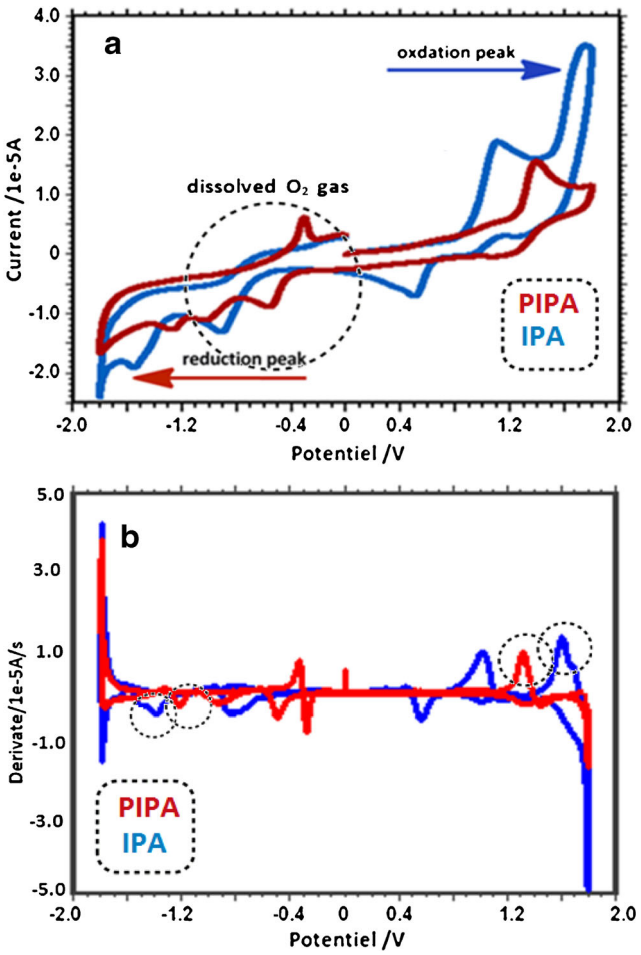

Fig. 6 Cyclic voltammograms of the IPA (**a**) and PIPA (**b**)

$$E'_g = E_{LUMO} - E_{HOMO} \quad (3)$$

To determine the oxidation and reduction potentials in voltammograms of the monomer and the polymer, the first derivative of voltammograms were plotted as a function of the potential. Examination of the first derivative of the CV for the compounds proved that one oxidation peak at 1.61 V and one reduction peak at −1.52 V for the monomer, and one oxidation peak at 1.32 V and one reduction peak at −1.22 V for the polymer were reached (Fig. 6b). Additionally, the calculated electrochemical band gaps agreed with the optical band gap values; as a result of the polyconjugated structure, the polymer had lower band gap than that of the Schiff base.

Fluorescence Characteristics

Fluorescence spectrum of Schiff base-phenyl acetylene and its corresponding polymer are given in Figs. 7 and 8. Slit with was set to be 5 nm in all fluorescence measurements. As seen in Fig. 7, the polymer turned into green while the color of its monomer was unchanged when looked under UV lamp with a wavelength at 366 nm by dissolving both monomer and polymer in aqueous solution of KOH. When polymer were excited with a light of 366 nm the maximum emission wavelength

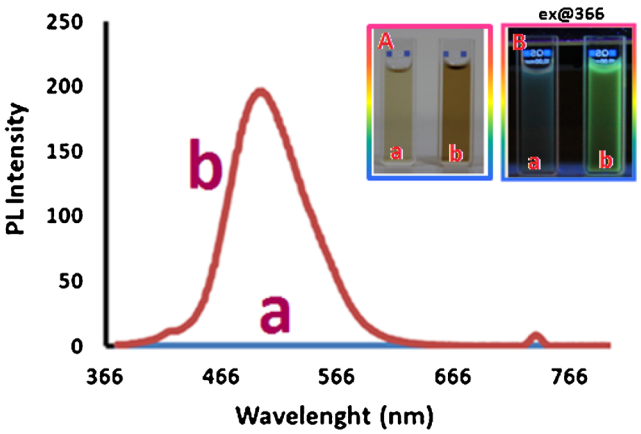

Fig. 7 Emission spectra of daylight of IPA (**a**) and PIPA (**b**) A] under UV lamp of IPA (**a**) and PIPA (**b**) B] Slit width: λ_{Ex} 5 nm, λ_{Em} 5 nm; concentration of the compounds: 0.01 mg/ mL

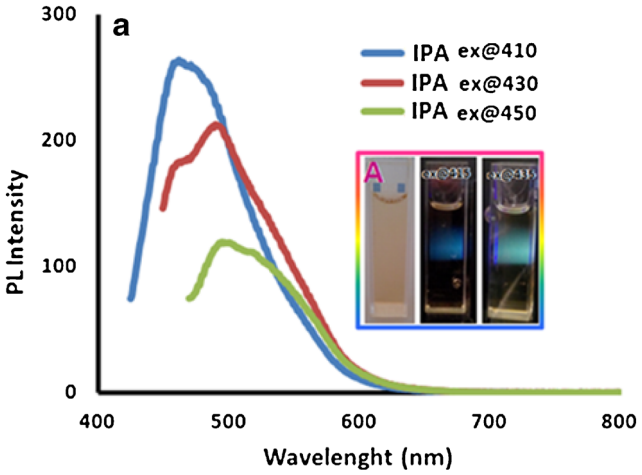

Fig. 8 Emission spectra of IPA (**a**) and PIPA (**b**) at different wavelengths, Slit width: λ_{Ex} 5 nm, λ_{Em} 5 nm; concentration of the compounds: 0.01 mg/ mL

was found to be 500 nm with an intensity of 197, and that fluorescence intensity was observed to be zero for the monomer. Stoke shift and FWHM values of the polymer were found to be 134 and 78 nm, respectively. As seen in Fig. 8, when both monomer and polymer were stimulated with a visible wavelength, both of them had fluorescence intensity, but polymer (Fig. 8b) had a higher level than that of the monomer (Fig. 8a). As seen in Fig. 8, fluorescence intensities of both monomer and polymer decreased as the wavelength increased. The wavelength and the intensity related to the maximum emissions are given in Table 2. When excited at 410 and 430 nm, the monomer emitted blue and green fluorescence light with an emission intensity of 260 and 213, respectively. The polymer emitted green light at 500 and 502 nm with an emission intensity of 374 and 203 when excited with 410 and 450 nm. The polymer emitted green light when excited with an excitation wavelength of 366 nm under UV light. The fluorescence quantum yields of polymer were calculated to be 9 and

Table 2 Fluorescence spectral data of the synthesized compounds with optimum concentrations in THF solvent

Compounds	λ_{Ex}			
		410	430	450
IPA	$I_{max(Em)}$	260	213	119
	$\lambda_{max(Em)}$	468	491	497
PIPA	$I_{max(Em)}$	374	203	52
	$\lambda_{max(Em)}$	500	502	507

λ_{Ex} Excitation wavelength for emission, $\lambda_{max(Em)}$ Maximum emission wavelength, $I_{max(Em)}$ Maximum emission intensity

14 % in the UV (366 nm) and visible area (410 nm), respectively [20, 21].

Electrical Conductivities

The current–voltage plotted regarding to the solid state conductivity values measured for the synthesized polymer at nitrogen atmosphere and the results are given in Fig. 9. The measurements for the polymer were carried out in pure form

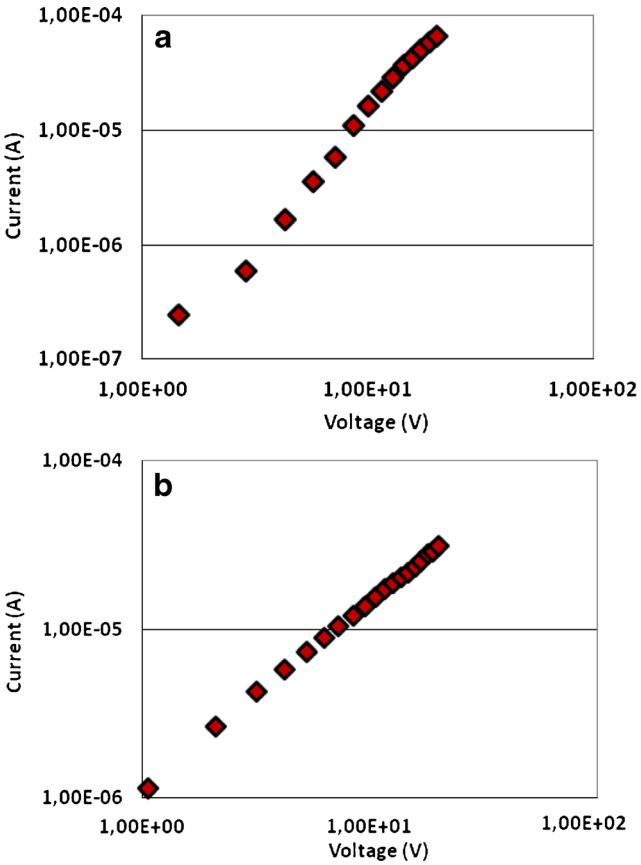

Fig. 9 Current–voltage graph before doped (**a**) after 24 h doped (**b**) of PIPA

then, the polymer were exposed to iodine vapor in a desiccator, and the change in their conductivities versus time was measured at specific time intervals (2 h, 5 h, 10 h, 24 h, vs.) by doping. There was no observable change in current values by changing the applied voltage before and after PIPA was doped, resulting in having a direct proportion between voltage and current as an evidence of ohmic resistance. Consequently, conductivity values were calculated to be 5.26×10^{-6} and 5.27×10^{-6} S cm^{-1} before and after iodine doping, respectively [22, 23].

In doping process, electron donor amine nitrogen and electron acceptor iodine were coordinated and the formation of radical cation (polaron) structure in polymer chain (on amine nitrogen) was enabled. Electron vacancy formed due to the polaron formation facilitated electron flow resulting in an increase in electrical conductivity. High electron intensity allowed the polymer to coordinate with iodine and consequently, electron flow increased at a higher level was obtained. Delocalization of π–conjugation was achieved through a combination of imine and acetylene functional groups in the polymer structure.

Thermal Analysis

Thermal decomposition steps of IPA and PIPA are given in Fig. 10. Thermal analysis curves to determine T_{20}, T_{50}, T_{on} temperatures and the number of decomposition steps, the exothermic and endothermic peaks for the monomer and polymer as well as the glass transition temperature (T_g) of polymer are given in Table 3. According to Table 3, initial decomposition temperature of the monomer was found to be higher than that of the polymer due to the formation of C-O etheric bond during the OP reaction (C-O-C coupling). Initial degradation temperatures (T_{on}) of the monomer and its polymer were obtained to be 185 and 190 °C, respectively. IPA and PIPA lost 20 % of their initial weights at 234 and 753 °C; and the temperatures corresponding to 50 % weight losses were observed at 480 and 869 °C for IPA and PIPA, respectively. Additionally, the char % amounts at 1000 °C listed in Table 3, indicating that the maximum value of 52 % was obtained for PIPA which was highly thermostable. TG results revealed that

Table 3 Thermal degradation values of the synthesized compounds

Compounds	IPA	PIPA
[a]T_{on}	185	190
[b]$W_{max.}T$	249, 339	179, 216
20 % weight Loss	234	753
50 % weight Loss	480	869
% char at 1000 °C	34	52
DTA (exo/endo)	–/–	–/–
DSC [[c]T_g (°C) / [d]ΔCp (J/g)]	–/–	174/0.638

[a] The onset temperature

[b] Maximum weight temperature

[c] Glass Transition Temperature

[d] Change of specific heat during glass transition

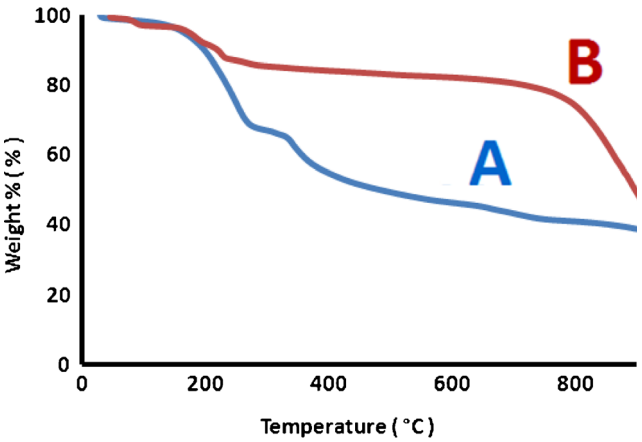

Fig. 10 TG curves of IPA (**a**) and PIPA (**b**)

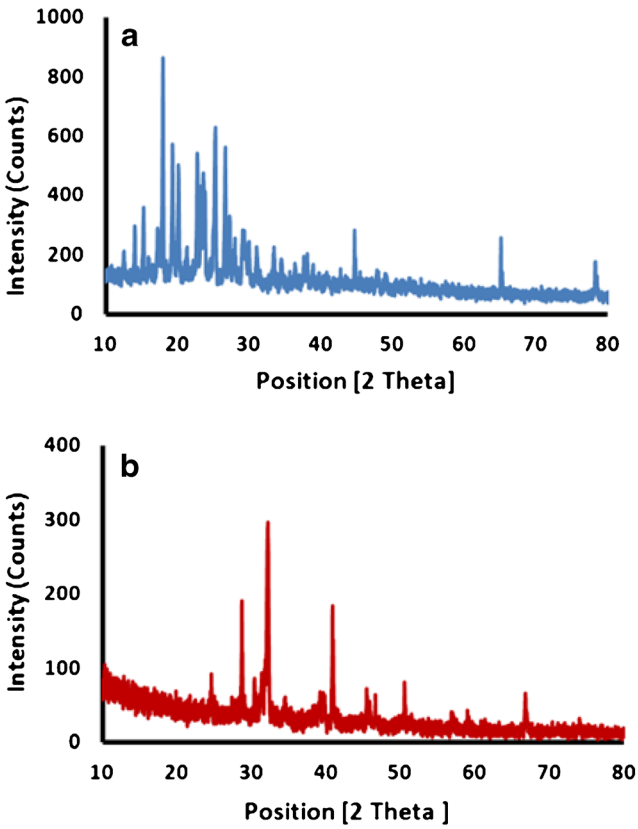

Fig. 11 XRD patterns of IPA (**a**) and PIPA (**b**)

Table 4 X-RD parameters of monomer and polymer

Compounds	Peak pos. [°2Th]	β (B obs. [°2Th])	Cos θ	Crystallite size [nm]
Five major peaks of the monomers	18.016	0.128	0.95	11.43
	19.342	0.128	0.94	11.55
	22.802	0.154	0.92	9.81
	25.313	0.179	0.90	8.62
	26.691	0.154	0.89	10.14
Five major peaks of the polymer	28.705	0.128	0.87	12.48
	32.134	0.128	0.85	12.77
	40.881	0.154	0.76	11.87
	50.545	0.154	0.64	14.10

the polymer with a long conjugated π–band increased the delocalization of π electrons, leading to a higher resistance against temperature. Glass transition temperature (T_g) of the synthesized polymer was found to be lower than glass initial decomposition temperature (T_{on}) as expected.

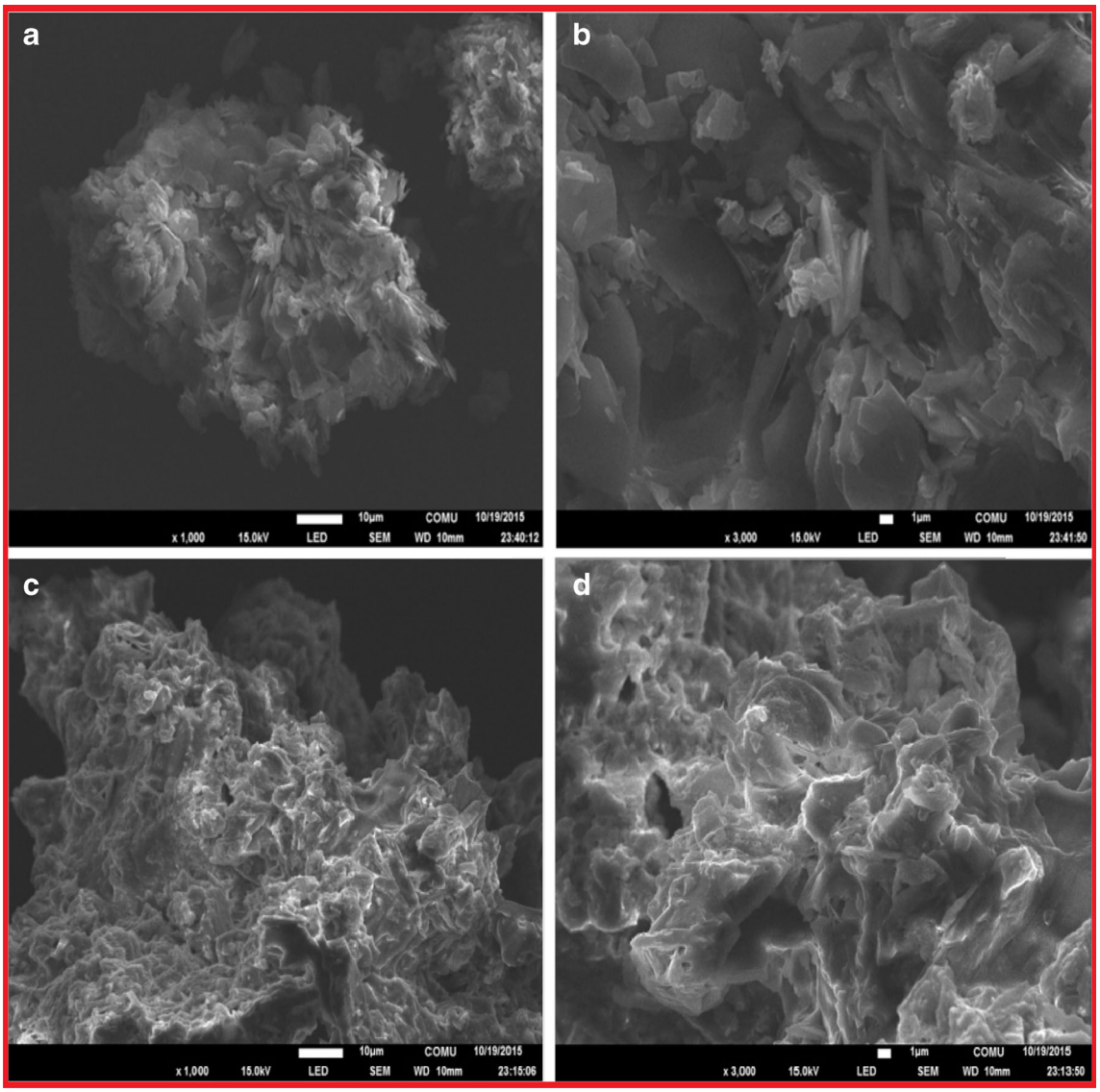

Fig. 12 SEM photographs 10 μm and 1 μm of IPA (**a**–**b**) 10 μm and 1 μm of PIPA (**c**–**d**)

X-Ray Diffraction (X-RD)

Figure 11 shows the X-RD patterns of imine-phenyl acetylene and its polymer. A decrease in the crystallinity rate was observed from 33 to 19 % for the Schiff base monomer and the polymer, respectively. The reason could be attributed to the loss of peaks between 2θ values of 10 and 30, when Fig. 11 was analyzed. Using the diffraction data, the mean crystallite sizes of the monomer and the polymer, D, were determined according to the Scherer equation $D = (0.9\lambda) / (\beta.\cos\theta)$, where λ was X-ray wavelength (1.5406 Å), θ was Bragg diffraction angle, and β was the full width at half maximum of the diffraction peak) [24, 25]. The average crystallite sizes of the monomer and the polymer are given in Table 4. The calculated D values gave information about the types of crystal structure and the interlayer distance.

Morphological Characterization

Surface morphological analyses for imine-phenylacetylene (IPA) and its polymer (PIPA) are given in Fig. 12. For IPA, nonhomogeneous flat structured particles were observed as it got closer to the surface. For PIPA, the particles were seen to be more corrugated and interlocked homogeneous structures.

Conclusion

A conjugated polymer was synthesized containing both acetylenic and imine functional groups in the structure. The monomer and polymer were spectroscopically characterized. The synthesized imine-phenyl acetylene polymer was found to be fluorescent due to the imine portion of the molecule dominating the electronic transitions and some contribution from the aryl acetylene moiety. Low level electronic structure calculations on models of these compounds also showed that the π-electrons in the combined imine/acetylene systems were delocalized over both functional groups. Consequently, the increase in the conductivity of the substance gave a possible usage as the semi-conductive polymer in electronic, opto-electronic and photovoltaic applications. TG results revealed that the polymer with a heat resistant property was successfully synthesized.

Acknowledgments The authors thank Çanakkale Onsekiz Mart University scientific research project commission for support with the project number (Project Nu.: FBA-2015-490).

References

1. Skotheim TA (1986) Interfaces between electronically and ionically conducting polymers: applications to ultra high-vacuum electrochemistry and photoelectrochemistry. Synth Met 14:31–43
2. Ferraro JR, Williams JM (1987) FT-IR micro-spectroscopic studies of several charge-transfer organic electrical conductors. Appl Spectrosc 41:1377–1382
3. Korshak YV, Medvedeva TV, Ovchinnikov AA, Spector V (1987) Organic polymer ferromagnet. Nature 326:370–372
4. Masuda T, Isobe E, Higashimura T, Takada K (1983) Poly[1-(trimethylsilyl)-1-propyne]: a new high polymer synthesized with transition-metal catalysts and characterized by extremely high gas permeability. J Am Chem Soc 105:7473
5. Masuda T, Higashimura T (1986) Polyacetylenes with substituents-their synthesis and properties. Adv Polym Sci 81:121–165
6. Asdente A, Ottoboni A, Furlani A, Russo MV (1991) The influence of humidity on the electrical conductivity of iodine doped polyphenlacetylene. Synth Met 41:89–90
7. Furlani A, Iucci G, Russo MV, Bearzotti A, Amico RD (1992) Iodine-doped polyphenylacetylene thin-film as a humidity sensor. Sensors Actuators B Chem 8:123–126
8. Hann RA, Bloor D (1989) Organic materials for nonlinear optics. Spec Publ Roy Soc Chem London, 69
9. Neher D, Wolf A, Bubeck C, Wegner G (1989) Third-harmonic generation in polyphenylacetylene: exact determination of nonlinear optical susceptibilities in ultrathin films. Chem Phys Lett 163:116–122
10. Tada K, Sawada H, Kyotane J, Yoshino K (1995) Optical properties of perfluoroalkylated poly(diphenylacetylene). Jpn J Appl Phys 34:1083–1085
11. Kaya İ, Yıldırım M, Kamacı M (2009) Synthesis and characterization of new polyphenols derived from o-dianisidine: the effect of substituent on solubility, thermal stability, and electrical conductivity, optical and electrochemical properties. Eur Polym J 45:1586–1598
12. Kaya İ, Bilici A (2007) Synthesis, characterization, thermal analysis, and band gap of oligo-2-methoxy-6-[(4-methylphenyl)imino]methylphenol. J Appl Polym Sci 104:3417–3426
13. Kaya İ, Kartal E, Şenol D (2015) Synthesis and characterization of polyphenol derived from Schiff bases containing methyl and carboxyl groups in the structure. Des Monomers Polym 18:524–535
14. Şenol D, Kaya İ (2014) Synthesis and characterization of aromatic compounds containing imine and amine groups via oxidative polycondensation. Des Monomers Polym 17:557–575
15. Colladet K, Nicolas M, Goris L, Lutsen L, Vanderzande D (2004) Low-band gap polymers for photovoltaic applications. Thin Solid Films 451–452:7–11
16. Kaya İ, Yıldırım M (2007) Synthesis, characterization, thermal stability and electrochemical properties of poly-4-[(2-methylphenyl)iminomethyl]phenol. Eur Polym J 43:127–138
17. Yıldırım M, Kaya İ (2009) Soluble semi-conductive chelate polymers containing Cr(III) in the backbone: synthesis, characterization, optical, electrochemical, and electrical properties. Polymer 50:5653–5660
18. Doğan F, Kaya İ, Temizkan K (2015) Template-free oxidative synthesis of polyaminonaphthol nanowires. Eur Polym J 66:397–406
19. Cervini R, Li XC, Spencer GWC, Holmes AB, Moratti SC, Friend RH (1997) Electrochemical and optical studies of PPV derivatives and poly (aromatic oxadiazoles). Synth Met 84:359–360
20. Doğan F, Kaya İ, Bilici A, Yıldırım M (2015) Chemical oxidative polymerization, optical, electrochemical and kinetic studies of 8-amino-2-naphthol. J Polym Res 22:104

21. Yıldırım M, Kaya İ (2012) Synthesis and characterization of iminothiazole bearing polyphenol with adjustable white–yellow photoluminescence color. Synth Met 162:2443–2450
22. Arafa IM, El-Ghanem HM, Bani-Doumi KA (2013) $PdCl_2$-Polyaniline composite for CO detection applications: electrical and optical response. J Inorg Organomet Polym 23:365–372
23. Pramanik S, Karak N, Banerjee S, Kumar A (2012) Effects of solvent interactions on the structure and properties of prepared PAni nanofibers. J Appl Polym Sci 126:830–836
24. Baranwal BP, Fatma T, Varna A (2009) Synthesis, spectral and thermal characterization of nano-sized, oxo-centered, trinuclear carboxylate-bridged chromium (III) complexes of hydroxycarboxylic acids. J Mol Struct 920:472–477
25. Kolmas J, Jaklewicz A, Zima A, Bucko M, Paszkiewicz Z, Sloarczyk A, Kolodziejski W (2011) Incorporation of carbonate and magnesium ions into synthetic hydroxyapatite: the effect on physicochemical properties. J Mol Struct 987:40–50